# AN ALTERNATIVE SUBGRID MODELING FOR LARGE-EDDY SIMULATIONS OF A HOMOGENEOUS ISOTROPIC TURBULENCE

**Luiz E. B. Sampaio, luizebs@mec.puc-rio.br**
**Angela O. Nieckele, nieckele@mec.puc-rio.br**
Department of Mechanical Engineering, Pontifícia Universidade Católica do Rio de Janeiro, Rua Marquês de São Vicente, 225 Gávea 22453-900 Rio de Janeiro - RJ - Brasil

***Abstract.*** *One of the key issues regarding Large-Eddy Simulations (LES) is the modeling of the interaction between the resolved and unresolved scales. The spatially filtered Navier-Stokes equation describing the evolution of the large scales includes a term representing that interaction, in the form of a divergence of a tensor, which cannot be closed and therefore must be modeled. Two possibilities have been extensively explored in the literature: while structural subgrid modeling strives to predict as accurately as possible that tensor, functional modeling tries to mimic only the dissipation of the energy arriving at the small scales. The vast majority of functional subgrid models currently employed in LES makes use of a diffusive formulation – the eddy-viscosity assumption – by which the tensor is supposed aligned with the symmetrical part of the velocity gradient, which is generally not true. Since the term to be modeled arises from an algebraic manipulation of an advective term, the purpose of this paper is, therefore, to investigate and validate an alternative subgrid modeling, based on an advective formulation. In such approach, instead of modeling the tensor and take its divergence, one aims directly at the "subgrid force", which has only tree components. This force is built in a way to comply with two basic principles: it must act only in the smallest scales, and it must be of advective nature, which means it must have a preferred direction, aligned with the mass flux. The results for benchmark test cases involving forced and decaying Homogeneous Isotropic Turbulence show that this approach can successfully represent the small scale structures, while guaranteeing numerical stability and greater robustness in non-uniform mesh environments, when compared to traditional eddy-viscosity based models.*

***Keywords:*** *turbulence, Large-Eddy Simulations, subgrid model*

## 1. INTRODUCTION

Modeling the interaction between the resolved and unresolved scales is the main objective of Large-Eddy Simulations (LES). The spatially filtered Navier-Stokes equation describing the evolution of the large scales includes a term representing that interaction, in the form of a divergence of a tensor, which cannot be closed and therefore must be modeled. Two possible approaches are extensively explored in the literature (Sagaut, 2002): functional modeling and structural modeling. In the former, one aims to represent the role of the small scales in the dissipation of the turbulence energy being transferred by the well-known energy cascade. In this case, no effort is made to match the sub-grid tensor prediction to a Direct Numeric Simulation (DNS) data, which may be satisfactory as long as the correct rate of dissipation of energy is provided. In the latter case (structural modeling), the goal is to predict as exactly as possible the sub-grid tensor, which is normally done by extrapolating information contained in the neighbor scales.

The vast majority of functional subgrid models currently employed in LES (Smagorinsky, 1963, Germano et al., 1991) makes use of a diffusive formulation – the eddy-viscosity assumption – by which the tensor is supposed aligned with the symmetrical part of the velocity gradient, which is generally not true. This alignment is obtained by multiplying the strain rate by a scalar, known as eddy-viscosity, which may be derived from a characteristic length and a characteristic velocity. The characteristic length is readily available from mesh spacing, and usually is taken as the cubic root of the volume of the cell – control volume in the Finite Volume Method (FVM) case. While this seems appropriated for isotropic regular meshes, it is easy to understand its limitations when dealing with highly anisotropic ones.

Unlike functional subgrid models, in which the added viscosity action helps stabilizing the numerical scheme, most structural models (Bardina, et al., 1980, Sagaut, 2002), suffers from instability problems, and are generally used together with some eddy-viscosity based model, in a mixed formulation.

Since the term to be modeled arises from an algebraic manipulation of an advective term, the objective of this paper is, therefore, to investigate and validate an alternative subgrid modeling, based on an advective formulation, in regard to the prediction of "turbulence in a periodic box". In such approach, instead of modeling the tensor and take its divergence, one aims directly at the "subgrid force", which has only tree components. This force is built in a way to comply with two basic principles: it must act only in the smallest scales, and it must be of advective nature, which means it must have a preferred direction, so that smallest structures aligned with the mass flux are eliminated first (or faster). The performance of the model is tested employing both isotropic and anisotropic meshes to predict the "periodic box" in a way to cover more realistic cases without adding further complexity to the test problem.

## 2. SUBGRID MODELLING

The Navier-Stokes and continuity equations for incompressible flows are:

$$\frac{\partial \mathbf{u}}{\partial t} + \nabla \cdot (\mathbf{u}\,\mathbf{u}) = -\nabla p + \nu \nabla^{\mathbf{2}} \mathbf{u} \qquad , \qquad \nabla \cdot \mathbf{u} = \mathbf{0}\,, \tag{1}$$

with $\mathbf{u}$ the velocity, $p = P/\rho$ the modified pressure which incorporates the fluid density $\rho$, and $\nu$ the kinematic viscosity of the surrounding fluid.

To reduce the number of degrees of freedom of the original transport equations, the Large-Eddy Simulation (LES) method employs a spatial filtering operator to select the largest and most energetic structures to be computed, leaving only the small eddies to be modeled.

The filtered transport equations can be written as,

$$\frac{\partial \overline{\mathbf{u}}}{\partial t} + \nabla \cdot (\overline{\mathbf{u}}\,\overline{\mathbf{u}}) + \varepsilon_{\mathbf{com}} + \nabla \cdot \tau_{\mathbf{SGS}} = -\nabla \overline{p} + \nu \nabla^{\mathbf{2}} \overline{\mathbf{u}} \qquad , \qquad \nabla \cdot \overline{\mathbf{u}} = \mathbf{0}\,, \tag{2}$$

where $\overline{\mathbf{u}}$ is the filtered velocity, and $\overline{p}$, the filtered modified pressure. The commutative error, $\varepsilon_{com}$, often neglected, is a consequence of commuting the filtering process with a spatial derivative operator, while the subgrid tensor, $\tau_{SGS}$, is the result of commuting the filtering with the product $\overline{\mathbf{u}}\,\overline{\mathbf{u}}$ and needs to be modeled.

The vast majority of subgrid models (Sagaut, 2002), in particular the eddy-viscosity models, tries to capture only the forward energy cascade, where energy from the large eddies is transferred to small turbulent structures. In the continuous dynamic system, as found in the real world, the energy is dissipated at very small scales where viscous dissipation becomes important. However, in a simulation environment, there is a limit on the smallest mode a mesh can represent, and, unless a Direct Numerical Simulation (DNS) is used, the mesh is generally bigger than the scale at which dissipation is strong enough to end the energy cascade. In order to prevent the accumulation of energy in the smallest modes, we thus need to add a dissipative term, which is usually done by modeling the subgrid tensor $\tau_{SGS}$ as

$$T_{SGSij} = \tau_{SGSij} - \frac{1}{3}\,\tau_{SGSkk}\,\delta_{ij} = -2\,\nu_{SGS}\,\overline{S}_{ij} \quad ; \qquad \overline{S}_{ij} = 0.5\left(\frac{\partial \overline{u}_i}{\partial x_j} + \frac{\partial \overline{u}_j}{\partial x_i}\right), \tag{3}$$

where $T_{SGSij}$ is the trace-free tensor, $\nu_{SGS}$ is the subgrid viscosity, which is the essence of the SGSM, and $\overline{S}_{ij}$ is the filtered strain rate.

In the particular case of Finite Volume Method (FVM), the filtering operation may be conveniently confused with the volume integral over the control volume. Therefore, no further filtering is needed, and this process is said to be implicit, or embedded in the FVM.

### 2.1 Motivation for the advective formulation

As previously mentioned all eddy-viscosity models are based on an extra dissipative term added to the transport equations with the purpose of eliminating or damping the small structures, which would otherwise be fed and amplified by the energy cascade. The success of a LES resides mainly in the correct choice of the dissipative coefficient $\nu_{SGS}$ so that just enough dissipation is provided to damp the smallest modes, without over damping other structures that might be important, either because they already carry a significant percentage of the total turbulent energy, or because they play a significant role in the formation of other structures. In this context, the best one can expect from a eddy-viscosity sub-grid model is achieved when some kind of feedback control mechanism, such as the Germano et al. (1991) dynamic approach, is employed, which decreases the subgrid dissipation when the smallest modes are very weak and increases it when they become important. The dynamic model was originally proposed as a way to automatically adjust the coefficient present in the Smagorinsky sub-grid model (Smagorinsky, 1963), optimizing it for different flow regime requirements, a procedure that is, in principle, extensible to any other "static" model. Although the original idea was that the sub-grid coefficient should not vary when two different filter bandwidths are employed, latter, Germano (1999) showed that the model could be reinterpreted as a control feedback mechanism forcing the smallest resolved modes to have a fixed percentage of the energy contained in the adjacent frequencies. Apart from suffering from numerical instability (Sagaut, 2002), the dynamic model is still somewhat sensitive to mesh anisotropy, as all scalar eddy-viscosity approaches.

As an alternative idea to the widely accepted Boussinesq hypotheses (Eq. 3), we propose a new SGSM approach, which consists of enforcing the sub-grid damping by adding to the transport equations an additional force, i.e., $\mathbf{f} = \nabla \cdot \tau_{SGS}$. Instead of finding an expression for $\tau_{SGS}$ and adding its divergence to the Navier-Stokes equation, one can directly derive

a force $\mathbf{f}$ such that the smallest – or "spatially" fastest – modes supported by the mesh are severely damped, while those with twice their wavelength are almost or completely untouched.

A potentially advantageous effect of damping small modes is that the resulting discrete dynamic system is more robust and less prone to numerical instability. Generally, LES practitioners employ non-dissipative central difference schemes to calculate derivatives, avoiding other more stable approaches like upwind. Since instability issues are often related to constraints not allowing the use of a regular mesh, the above mentioned effect might prove handy, allowing more flexibility in mesh design. In fact, Sampaio (2006) have shown that the methodology presented here is very robust, even in highly stringent mesh environment presenting strong shrinking and stretching.

### 2.2 Advective formulation methodology

Without any lost of generality, the methodology is illustrated for a pure advection, 1-D case, for a scalar variable $\phi$ obeying the transport equation:

$$\frac{\partial \phi}{\partial t} + \mathbf{u} \cdot \nabla \phi + f_\phi = 0\,, \tag{4}$$

where $f_\phi$ is the "artificial" force to be derived, for a general scalar variable $\phi$. Later, the methodology will be extended to a more interesting case of a 3-D vector field, where $\phi$ is the velocity components, in a full Navier-Stokes equation.

The first step toward the derivation of a force capable of selectively damping only the smallest modes supported by the mesh is the identification of a fundamental difference between these modes, hereby referred to as undesired or cut-off modes, and smoother modes, of bigger wavelengths. A possible way to distinguish them is through the evaluation of the projected gradients of the transported variable $\phi$, at the faces of a control volume. In the mesh shown in Fig. 1, the gradient at the cell-center $A$, can be calculated using, for instance, Gauss theorem as

$$(\nabla \phi)_A = \frac{1}{V_A} \sum_{i=1}^{N_A} \phi_i \, \mathbf{S}_{F_i}, \tag{5}$$

where $V_A$ is the volume of the cell, $N_A$ is the number of faces of control volume $A$, $\phi_i$ is the transported variable evaluated at face "$i$", and $\mathbf{S}_{F_i}$ is a vector orthogonal to the face "$i$", pointing outwards from the cell, with magnitude equal to the face area.

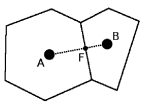


Figure 1. General mesh topology

For the projection of the gradient into the line segment $\mathbf{AB}$, at the face $F$ of Fig. 1, two possibilities are thus available: it can be obtained from the interpolations of the gradients at the two neighbor cell centers to the face,

$$\mathbf{AB} \cdot (\nabla \phi)_{\mathbf{int}} = \mathbf{AB} \cdot \frac{||\mathbf{BF}||(\nabla \phi)_A + ||\mathbf{AF}||(\nabla \phi)_B}{||\mathbf{AB}||}\,, \tag{6}$$

or alternatively, from the difference of the transported variable over the distance between cell centers,

$$\mathbf{AB} \cdot (\nabla \phi)_{\mathbf{n}} = \phi_B - \phi_A\,. \tag{7}$$

Equations 6 and 7 are presented in a general 3-D form and can be used in any topology, including unstructured meshes, where $\mathbf{AB}$ denotes the vector from point $A$ to point $B$, $||\mathbf{BF}||$ and $||\mathbf{AF}||$ are the distances from point $A$ and $B$ to the face $F$, respectively. The subscripts $A$ and $B$ refer to the points where gradients are evaluated whereas $\mathbf{int}$ and $\mathbf{n}$ identify how those face gradients are calculated. Additionally, an error $\varepsilon_\nabla$ can be defined as the difference between the two alternative ways of evaluating the gradient projected along $\mathbf{AB}$, at the face:

$$\varepsilon_\nabla \triangleq \mathbf{AB} \cdot \left[(\nabla \phi)_{\mathbf{n}} - (\nabla \phi)_{\mathbf{int}}\right]\,. \tag{8}$$

In the case of cell centered variables, the gradient at the centroid cannot capture the fastest spatial oscillating modes, but the face gradient constructed from the two neighbor's difference can. This is why central difference based schemes cannot detect and react to the presence of the smallest modes supported by the mesh. Those modes are thus allowed to grow and are the main source of numerical instability, unless some form of artificial damping is provided.

Examining Fig. 2(a), it can be seen that both methods provide the same results for a regularly spaced mesh for a smooth mode, which can be fitted by a second degree polynomial. On the other hand, for the fastest supported mode, as shown in Fig. 2(b), the error $\varepsilon_\nabla$ is significant and gets bigger as the amplitude of the spatial oscillations is increased. The same happens for modes whose wavelength spans at least four control volumes (Fig. 2(c)), where the derived force would also be non-zero, but a way to avoid this and restrict the action of this force to just the smallest mode will be shown later. Therefore, $\varepsilon_\nabla$ is an excellent candidate for detecting and indicating how much energy an undesired mode carries and can be used in the derivation of the force $f_\phi$.

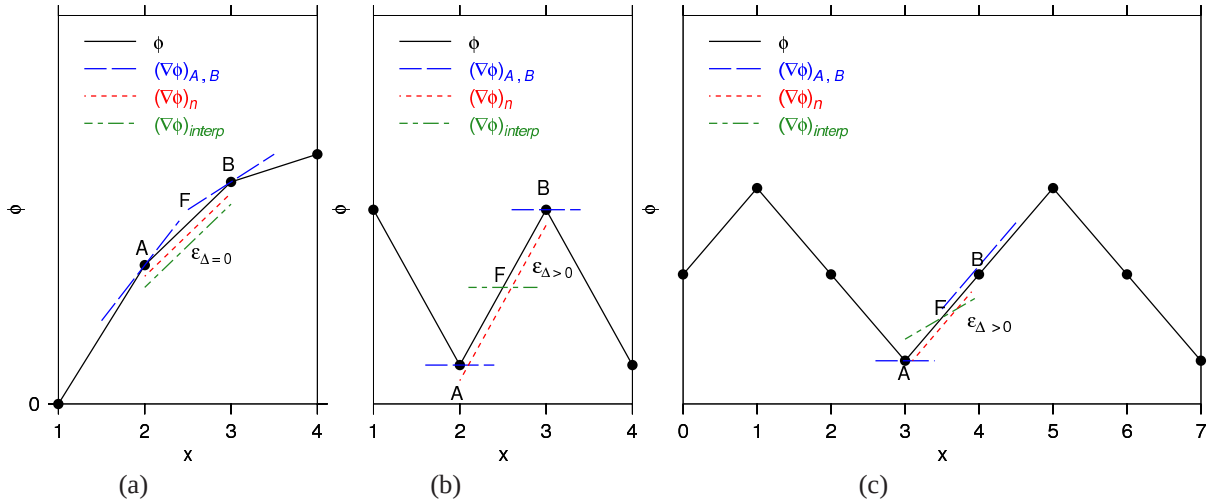


Figure 2. Different Gradient evaluations for: (a) a cut-off mode; (b) a 2nd degree polynomial mode; (c) a mode with twice the wavelength of the cut-off mode

Assuming that the gradient is based on a centered difference, using only nearest neighbors, the computational kernel involved in the 1-D case calculations spans 4 cell centers around the face. For a regular mesh, the error $\varepsilon_\nabla$ will be zero if values of the transported variable at cell centers can be fitted with a polynomial of degree less than or equal to 2, but this is not the case for higher order polynomials. Therefore, a force $f_\phi$ based on this gradient difference will not attenuate a zero$^{th}$, first or second order polynomial, which is a distinguishing feature when compared to current solutions to deal with numerical instability of non-dissipative schemes. An upwind scheme, for instance, will, for the same second order polynomial, yield a resultant force, altering the Navier-Stokes equation by adding a dissipative term.

The suitability of $\varepsilon_\nabla$ to build the force $f_\phi$ can be further appreciated by noticing that, being a gradient, it is almost in a form of an advection term, missing only a velocity factor. The amount of attenuation this force must provide to the variable $\phi$ can be seen from the expected advection of the scalar field, depicted in Fig. 3. In this figure, during the interval $\Delta t$, the fluid occupying positions $A$ and $B$ would have moved to new positions $A'$ and $B'$ respectively.

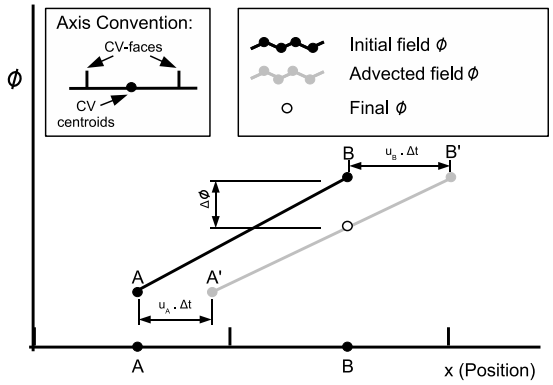


Figure 3. Advection of scalar field $\phi$ in a non-uniform velocity field

One can easily check in Fig. 3 that the decreasing in $\phi$ at cell center $B$, due to the advection of the piece-wise element connecting points $A$ and $B$, depends on the gradient $\nabla\phi_\mathbf{n}$ at its upwind face $F$, and the distance traveled by the neighbor centroids under advection, $\mathbf{u}_A\Delta t$ and $\mathbf{u}_B\Delta t$. Since the force must only complement the information captured by the "smooth" interpolated gradient $(\nabla\phi)_\mathbf{int}$, generally already present in discretized equations, we use $\varepsilon_\nabla$ instead of $\nabla\phi_\mathbf{n}$ to

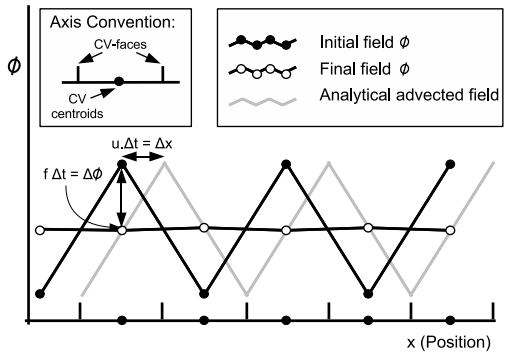


Figure 4. Damping of scalar field $\phi$ after advection by half control volume

derive the force:

$$f_{\phi_{F_i}} = \frac{\Delta\phi}{\Delta t} = -\frac{(\mathbf{AB}\cdot\mathbf{u}_B)\,\varepsilon_\nabla}{||\mathbf{AB}||^2 + \mathbf{AB}\cdot(\mathbf{u}_B - \mathbf{u}_A)\Delta t}\,. \tag{9}$$

Here, $f_{\phi_{F_i}}$ is the force associated with the centroid $B$, due to the influence of the upwind face $F_i$.

In 2-D or 3-D meshes, there are several faces that contribute to the force acting in a single control volume, and we need to find out which are upwind faces and how to weight their importance. In this paper, this is done by measuring the alignment of each face with the stream, through the variable

$$w_{F_i} = \mathbf{max}\left[\mathbf{u}\cdot\mathbf{ab}, 0\right] \quad ; \quad \mathbf{ab} = \frac{\mathbf{AB}}{||\mathbf{AB}||}, \tag{10}$$

where the subscript $F_i$ denotes the *i-th* face of the given control volume and $\mathbf{ab}$ is the normalized $\mathbf{AB}$ segment, pointing toward the cell center in question. Note that $w_{F_i}$ is greater than zero only for upwind faces, and that the bigger values are those corresponding to faces perpendicular to the stream.

Summing all contributions (Eq. 9) to the final force, $f_\phi$, using weighting factors as in Eq. 10, we get:

$$f_\phi = \frac{\sum_{i=1}^{N_{faces}} w_{F_i} f_{\phi_{F_i}}}{\sum_{i=1}^{N_{faces}} w_{F_i}}\,, \tag{11}$$

where $f_{\phi_{F_i}}$ is given in Eq. 9, $N_{faces}$ is the number of faces enclosing the given control volume, and $w_{f_i}$ are the non-normalized weighting factors.

As can be readily seen in Fig. 4, in this particular case, the undesirable mode damping characteristic time is of the order of the half control-volume advection time, or the time it takes a fluid element to be advected from the center of control volume to the face.

A significant improvement to this scheme may be obtained noticing that the gradient calculated according to Eq. (7) reaches its maximum accuracy at the midpoint of the line segment $\mathbf{AB}$, and not at the point where it cuts the face. Therefore, it is more accurate to select $\mathbf{AB}$'s midpoint as the target point for the interpolation of Eq. (6), instead of the point where $AB$ crosses the face, so that

$$\mathbf{AB}\cdot(\nabla\phi)_{\mathbf{int}} = \mathbf{AB}\cdot\left[(\nabla\phi)_A + (\nabla\phi)_B\right]/2\,. \tag{12}$$

Referring again to Fig. 2, another interesting feature to be explored is that, for the fastest mode (Fig. 2(a)), the face gradient calculated with Eq. (7) lies outside the range defined by the neighborhood centroid-evaluated ones, at points $A$ and $B$. This does not happens for the other modes (Fig. 2(b) and (c)).

Based on that, the action of the force can be really restricted to just the cut-off mode by setting $\varepsilon_\nabla$ to zero whenever $\mathbf{AB}\cdot(\nabla\phi)_n$ is inside the range limited by the values of $\mathbf{AB}\cdot(\nabla\phi)_A$ and $\mathbf{AB}\cdot(\nabla\phi)_B$. One can define a "switch" variable $\xi$, associated with each segment $\mathbf{AB}$, responsible for turning off the contribution of a smooth mode to the forcing term:

$$\xi_{AB} = \mathbf{max}\left\{\mathbf{sign}\left[\left(\frac{|g|}{|h|} - \beta_f\right),\, 0\right]\right\}\,, \tag{13}$$

where $\beta_f$ is an arbitrary tolerance, $\mathbf{sign}$ is a function returning $1$ or $-1$ for positive or negative arguments respectively, and $g$ and $h$ are given by:

$$g = \phi_A - \phi_B - \frac{1}{2}\,\mathbf{AB}\cdot\left[(\nabla\phi)_A + (\nabla\phi)_B\right] \quad ; \quad h = \mathbf{AB}\cdot\left[(\nabla\phi)_A - (\nabla\phi)_B\right]\,. \tag{14}$$

The weights $w_{F_i}$ thus become:

$$w_{F_i} = \xi_{AB}\ \mathbf{max}\left[\mathbf{u}\cdot\mathbf{ab}, 0\right]\ , \tag{15}$$

so that now the only faces contributing to the artificial force are those upwind of the control volume centroid, where the fastest mode supported by the mesh has been detected. Therefore, the only way we have a non-zero force in a volume is if one of its upwind faces presents a undesirable spacial oscillation aligned with the face normal vector $\mathbf{S}_{F_i}$

The ratio $|g|/|h|$ in Eq. (13) roughly indicates how much energy the cut-off mode contains compared to "smoother" modes. Therefore, $\beta_f$ defines a threshold for this ratio, when the "artificial" forcing term starts to act. Typical values of $\beta_f$ are between 1 and 2, and for $\beta_f > 1$, modes like the one depicted in Fig. 2c are no longer attenuated.

The application of the above methodology to the momentum equation is straightforward, sufficing to replace $\phi$ by the velocity vector field, $\mathbf{u}$.

It is expected that this new approach eliminates or attenuates the mesh instability even when central-differencing is used, allowing more flexibility in mesh spacing adapting, providing at the same time subgrid modeling functionality. However it is important to realize that it only represents the forward energy cascade, although in principle it should also be possible to use the same forcing term philosophy to implement corrections aiming to capture the backward cascade. As in Germano (1991), this model is dynamic in the sense that the growth of undesirable modes is immediately detected by the gradient error $\varepsilon_\nabla$, which in turn controls the forcing $f_\phi$ in such a way as to damp these modes, without attenuating smoother turbulent structures.

The idea of eliminating the smaller spatial modes in numerical simulations of turbulent flows, which is the essence of LES, is not new and several strategies have been proposed over the years. Apart from the widespread eddy-viscosity strategy, other possibilities include Fourier treatment of field variables from time to time to discard undesired modes or modes faster than a certain threshold (Fornberg, 1977). The idea of the proposed model is, in a sense, similar to the one proposed by Fornberg (1977), but a physical instead of a spectral space is used, allowing complex geometry applications with unstructured meshes. Furthermore, instead of a Fourier treatment done sporadically, we here opted for a continuous damping, acting at every time step.

## 3. RESULTS

The proposed sub-grid model was tested on a wide range of situations (Sampaio, 2006) including: 1D-transient scalar advective transport case; 2D steady-state scalar transport; and finally, a more realistic 3D turbulent in a box, or Homogeneous Isotropic Turbulence (HIT) governed by full Navier-Stokes equation. In this section we present only the results for the HIT, which are compared to those obtained with more traditional sub-grid models, as the Smagorinsky (1963) and dynamic (Germano et al., 1991).

The geometry consists of a unit-side cubic box with periodic conditions in all opposite faces, where two different situations are examined. Firstly, a pseudo-random body force acting only in the large scales is imposed, following Eswaran and Pope (1988), injecting energy and balancing the dissipation rate at small scales. The spectrum of energy is extracted after the flow has reached statistic steady-state, and compared to the theoretical $-5/3$ slope. In the second set of tests, the initial velocity field contains only very large scales, and the flow develops with no dissipation until the energy reaches the Kolmogorov scales, where the viscous forces become important. Once the cascade of energy reaches the dissipation range, the total kinetic energy of the box starts to decay logarithmically (Mansourt and Wray, 1993, Wang et al., 2000). As we will be using Large Eddy-Simulations in a coarse mesh instead of a DNS, the effect of molecular viscosity will be mimicked by the subgrid modeling, which means that the logarithm decay of energy should start as soon as the energy reaches not the Kolmogorov scales, but the smallest modes supported by the mesh.

### 3.1 Statistically steady-state of forced HIT

The Homogeneous Isotropic Turbulence (HIT) is obtained in a periodic box, by adding a forcing term to the filtered Navier-Stokes equation, as

$$\frac{\partial\overline{\mathbf{u}}}{\partial t} + \nabla\cdot(\overline{\mathbf{u}}\,\overline{\mathbf{u}}) + \mathbf{f_{SGS}} = -\nabla\overline{p} + \nu\nabla^{\mathbf{2}}\overline{\mathbf{u}} + \mathbf{f_b} \quad ; \quad \nabla\cdot\overline{\mathbf{u}} = \mathbf{0} \tag{16}$$

where $\mathbf{f_b}$ is a pseudo-random body force acting only in the largest scales, following exactly the proposal of Eswaran and Pope (1988). The subgrid term $\mathbf{f}_{SGS}$ is either $\nabla\cdot\tau_{SGS}$ for the traditional subgrid models or $\mathbf{f}$ for the advective approach proposed.

Since the primary purpose of this simulations is to evaluate the subgrid models, we set the viscosity to zero, which results in an unbounded Reynolds number. This, however, does not cause any instability in the simulations, thanks to the high wave numbers damping provided by the sub-grid modeling.

After statistical steady-state is reached, the energy spectrum is extracted from the velocity field. An extensive study of the influence of parameters $\alpha_f$ and $\beta_f$ in the spectrum has been performed and the most relevant results are shown in Fig.

5. The results suggested that for each $\beta_f$ there is one $\alpha_f$ that optimizes the spectrum in relation to the theoretical $-5/3$ slope. The spectra for the optimal pairs of parameters are shown in Fig. 5, where we can seen that all of them presents a slightly better agreement with the $-5/3$ relatively to the traditional dynamic subgrid model.

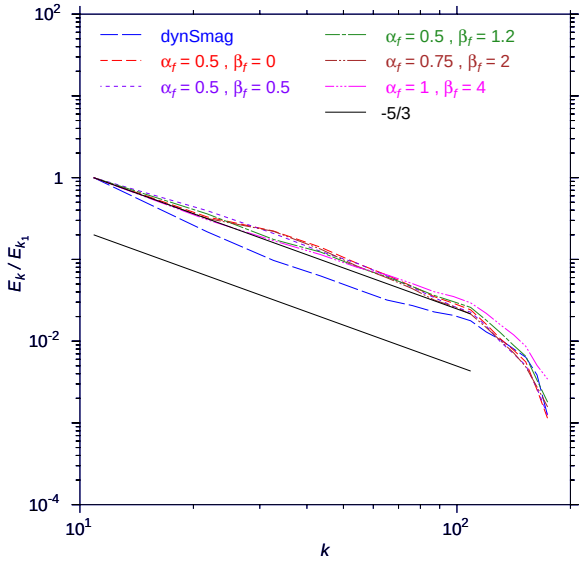


Figure 5. Spectrum of HIT in a periodic box with $32^3$ for optimal combinations of $\alpha_f$ and $\beta_f$.

### 3.2 Decaying Homogeneous Isotropic Turbulence

Turbulence is a complex phenomena that has many aspects, being the "universal" $-5/3$ spectrum just one of them. Therefore, an accurate spectrum result is not enough to guarantee that a new model will be successful in numerical simulations of turbulent flows. Another important behavior that turbulence simulations must be able to reproduce is the free decaying of kinetic energy and dissipation rate, which obeys a logarithmic law during a certain period of time (Mansour and Wray, 1993, and Wang et al., 2000). This is explored in this subsection for the same periodic box of Section 3.1, but here we initialize the velocity field with a spectrum given by

$$E(k) = E_a (k/k_0)^4 \exp(-2(k/k_0)^2)\,, \quad \text{with} \quad k_0 = 8 \quad \text{and} \quad E_a = 1000\,, \tag{17}$$

so that it contains only large structures, and let the flow evolve without any "pseudo-random" forcing ($\mathbf{f_b} = 0$). Initially, the energy stored in the largest scales is transfered to the neighborhood modes where there is still no dissipation. The total kinetic energy is thus kept constant, until the energy reaches the smallest modes supported by the mesh, when the subgrid modeling starts to act, damping the smallest structures. From this point on, the total kinetic energy ($\langle K \rangle$) decays logarithmically, as can be seen in Fig. 6(a) for the different subgrid models and different meshes. In the figures that follow, the legend code "f-LES" refers to the proposed forcing subgrid model, with parameters $\alpha_f = 0.5$ and $\beta_f = 1.2$.

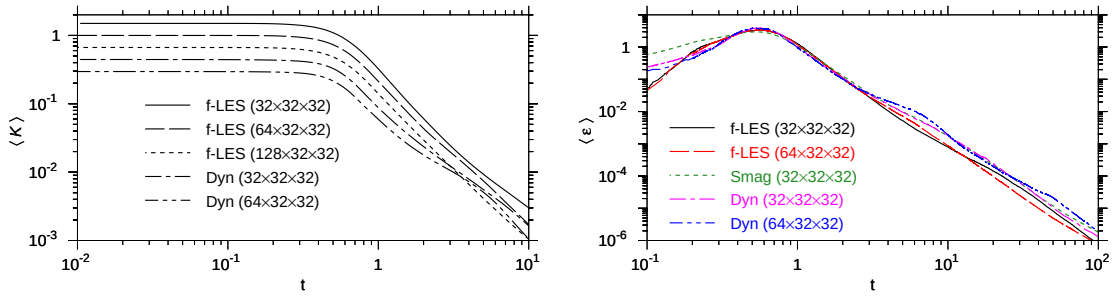


(a) (b)

Figure 6. Comparison of HIT LES behavior in isotropic and anisotropic meshes with different models: a) kinetic energy decaying; b) dissipation rate decaying.

In Fig. 6 (a), the curves for the different cases have been vertically shifted for better visualization, since all simulations started from the same initial velocity field, therefore with the same $\langle K \rangle$. All the subgrid models result in similar curves for the total kinetic energy, although the proposed strategy seems to present an extended logarithmic range.

The dissipation rate also obeys a logarithmic decay from the time the energy reaches the smallest scales on. Before this point, it is clear from Fig. 6(b) that the proposed subgrid model is less dissipative than both Dynamic and Smagorinsky, being the latter the most dissipative of all. Since the high frequency spectrum is empty in the beginning of the simulations and becomes populated as time goes by, one can conclude that the Smagorinsky model dissipates energy at larger scales when compared to Dynamic model and advective forcing, which act more selectively, damping only the smallest modes, as expected.

Figures 6(a) and (b) also present some results for the same models under anisotropic periodic box ($64 \times 32 \times 32$ and $128 \times 32 \times 32$), initialized with the same velocity field as before. The proposed advective subgrid formulation presents a more consistent behavior than traditional models when dealing with isotropic and anisotropic meshes, being the curves are almost coincident, which is very desirable.

## 4. FINAL REMARKS

A new approach to subgrid modeling has been proposed and investigated hoping to develop Large-Eddy Simulations more versatile and robust. The proposed formulation mimics an advective damping whose action is restricted to the smallest modes supported by the mesh, with no effect on other structures. The rationale for the forcing term has been presented and followed from the fact that the subgrid term in the filtered Navier-Stokes equation comes from the advective term, thus justifying our efforts to give the new proposal an advective nature.

The performance of the new proposal has been evaluated for the classic benchmark test cases involving forcing and decaying of homogeneous isotropic turbulence. The spectrum and decaying rates for kinetic energy obtained with the advective forcing proved to be very similar to those obtained with the dynamic model and therefore much better than those of Smagorinsky model. Since the dynamic model has its own issues, mostly regarding numerical instabilities, a new approach that presents similar automatic damping of small scales has a great potential. Our expectation around this new approach is further substantiated by other simulations (Sampaio, 2006) involving more complex cases not shown in this paper, which confirmed its robustness and immunity to numerical instabilities, even in a highly adverse mesh environment. The proposed model also showed a promising consistency in predictions when facing different mesh anisotropies, which suggests it can tackle more complex problems.

## 5. ACKNOWLEDGEMENTS

The authors acknowledge the support awarded to this research by the Brazilian Research Council, CNPq.

## REFERENCES

Bardina, J., Ferziger, J. H. and Reynolds, W. C., “Improved turbulence scale models for large eddy simulation”. AIAA Paper, 80–1357.

Eswaran, V. and Pope, S. B., 1988, “An examination of forcing in direct numerical simulations of turbulence”, Computers and Fluids, Vol. 16:3, pp. 257–278.

Fornberg, B., 1977, “Numerical study of 2-D turbulence”, Journal of Computational Physics, Vol. 25:1, pp. 1–31.

Wang, H., Sonnenmeier, J. R., Gamard, S. and George, W., 2000, “A contribution toward understanding DNS simulations of isotropic decaying turbulence using similarity theory”, Turbulence Research Laboratory, State University of New York at Buffalo, Buffalo, NY, USA.

Germano, M., Piomelli, U., Moin, P., and Cabot, W. H., 1991, “A dynamic subgrid-scale eddy viscosity model”, Physics of Fluids A, Vol. 3:7, pp. 1760–1765.

Germano, M., 1999, “From RANS to DNS: Towards a Bridging Model”, Direct and Large-Eddy Simulation III, Proceedings of the Isaac Newton Institute Symposium / ERCOFTAC workshop, Ed. P. Voke, N. Sandham, and L. Kleiser, Kluwer, Vol. 7, pp. 225–236.

Mansour, N. N. and Wray, A. A., 1993, “Decay of isotropic turbulence at low Reynolds number”,Physics of Fluids, Vol. 6:2, pp. 808–814.

Sagaut, P., 2002, “Large eddy simulation for incompressible flows, An introduction”, Springer.

Sampaio, L. E. B., 2006, “Large Eddy Simulations of the Thin Plate Separation Bubble at Shallow Incidence”, Ph. D. Thesis, Department of Mechanical Engineering, Pontifícia Universidade Católica do Rio de Janeiro, RJ, Brasil, in Portuguese.

Smagorinsky, J., 1963, “General circulation experiments with the primitive equations. I: the basic experiment”, Monthly Weather, Vol. Rev. 91:3, pp. 99–165.

## 6. Responsibility notice

The authors are the only responsible for the printed material included in this paper